Assessment of Changes in Wetland Storage in Gurupura River Basin of Karnataka, India, Using Remote Sensing and GIS Techniques

Subrahmanya Kundapura, Renuka Kommoju and Irshan Verma

Abstract In view of the significant importance of wetlands in the ecosystem and regional economy, an attempt has been made to analyze the impact of land use/land cover dynamics and other contributing factors on spatial status of Gurupura river basin wetland ecosystem located in Karnataka region. The impact assessment has been carried out by analyzing the multi-temporal changes in the storage capacities of wetlands in the watershed, by using remote sensing data of LISS-III. The multi-temporal land use/land cover statistics will reveal the significant changes that have taken place over time in the watershed. The runoff generated can be easily calculated from this information which gives an idea of the total input into the system. In response to these upstream watershed changes, wetland has exhibited changes in spatial extension, structure, and hydrological characteristics. As a consequence of continuously changing land use/land cover characteristics and unpredictability of the monsoon, the wet land ecosystems have exhibited considerable changes in spatial extent and their storage capacities. Overall, there has been degradation in the storage capacities of the wetland ecosystems of the region causing a multitude of adverse effects such as increase in floods and submergence of mainland.

Keywords Remote sensing · Wetland ecosystems · Land use/land cover

1 Introduction

Wetlands hold a vital role in the hydrological dynamic of a watershed. They are widely regarded as the 'kidneys' of the hydrological system, fittingly so, as wetlands play a major role in the ecosystem by providing an efficient way for sediment and toxic removal. By retaining the surface runoff and slowly discharging it back to the hydrological cycle, wetlands not only filter the sediment and toxic wastes but also

S. Kundapura (✉) · R. Kommoju · I. Verma
Department of Applied Mechanics and Hydraulics, National Institute of Technology Karnataka, Surathkal, India
e-mail: subrahmanyakundapura@gmail.com

provide opportunities for ground-water recharge and discharge, flood mitigation, and flow regulation. The filtering process reduces many problems of the likes of saltwater intrusion and increasing sediment deposits. Wetland systems also aid the process of nutrient cycling in the region. This is of prime importance for the vegetation growth in the region, and this vegetation further curbs the erosion process. Wetlands are also notorious for shoreline protection and acting as wind breaks to prevent erosion by wind [1, 2]. One of the most important aspects of wetlands is the amazing streak of wildlife finding habitat in these systems. Wetland systems are home to many species of migrating birds and other flora and fauna. Therefore, for the conservation of these flora and fauna, the conservation of wetlands becomes imperative [3].

In hydrology, a water balance equation can be used to describe the flow of water in and out of a system. A system can be one of several hydrological domains, such as a column of soil or a drainage basin or a wetland [4–6]. A general water balance equation is:

$$P = Q + E + \Delta S \tag{1}$$

where

P Precipitation
Q Runoff
E Evapotranspiration
ΔS Change in the storage

The basic hydrology of a wetland system can be related to any system with defined inputs and outputs. The inputs to a wetland system are the precipitation, the surface-water inflow, and the ground-water inflow. Evapotranspiration, surface-water outflow, ground-water outflow are the outputs from the system. The water balance equation for a wetland can be written as follows

$$P + \text{SWI} + \text{GWI} = \text{ET} + \text{SWO} + \text{GWO} + \Delta S \tag{2}$$

where P is precipitation, SWI is surface-water inflow, SWO is surface-water outflow, GWI is ground-water inflow, GWO is ground-water outflow, ET is evapotranspiration, and ΔS is change in storage [7–10].

To make an assessment in the changes in storage capacities, an effort has been made in this study to incorporate the input factor of surface-water inflow to give an idea of the changing situation. The surface-water inflow can be easily calculated by using remotely sensed data and the Soil conservation Services Curve Number (SCS-CN) method [11–13]. The SCS-CN is a simple, widely used, and efficient method for determining the approximate amount of runoff from a rainfall even in a particular area. Although the method is designed for a single storm event, it can be scaled to find average annual runoff values [14–16]. The stat requirements for this method are very low rainfall amount and curve number. The curve number is based on the area's hydrological soil group, land use, treatment, and hydrological condition [17, 18]. The former being of greatest importance.

2 Study Area

The Gurupura River or Phalguni River or sometimes Kulur River has its origins in the Western Ghats, which drains itself in the Arabian Sea at Mangalore. The New Mangalore Port (NMPT) and Mangalore Chemicals and Fertilizers are situated at the northern banks of Phalguni River. Once upon a time, it formed northern boundary of Mangalore city along with Netravati River as southern boundary. The study area chosen for this study is the entire Gurpur river basin. The complete area of the river basin is about 874.68 km^2 with the drainage length of the river being 52.31 km approximately. The complete basin lies between 12° 50′ 24″N and 13° 11′ 24″N latitude and 74° 45′ 0″E and 75° 21′ 0″E longitude as is shown in the figure. The basin area lies in the Survey of India (SOI) toposheet No. 48L/13/NW, 48L/13/NE, 48L/13/SE, 48L/13/SW.

3 Data Used

3.1 Rainfall

The rainfall data used for this study was obtained from Indian Meteorological Department (IMD). The dataset obtained was a $0.5° \times 0.5°$ daily rainfall dataset. The rainfall maps were prepared from this dataset under GIS environment by plotting the gridded rainfall data with the coordinate grid around the study area. Spatially interpolated maps of rainfall were prepared from the grid points containing rainfall information by applying Universal Kriging technique [19–21]. Maximum rainfall intensity is found in the study area in the month of July, in fact 30–35% of the total rainfall occurs in the month of July. Also there is an increase in rainfall in 2010 than 2003.

3.2 Soil Data

Soil maps in GIS compatible shapefile format were obtained from National Bureau of Soil Survey and Land Use Planning (NBSS&LUP) and Food and Agricultural Organization-UNESCO (FAO-UNESCO). By cross-referencing both the datasets, the derived product obtained was the hydrological soil group classification of the study area in the following four classes

- Group A: Soils in this group have low runoff potential when thoroughly wet. Water is transmitted freely through the soil. Group A soils typically have less than 10% clay and more than 90% sand or gravel and have gravel or sand textures.

- Group B: Soils in this group have moderately low runoff potential when thoroughly wet. Water transmission through the soil is unimpeded. Group B soils typically have between 10 and 20% clay and 50–90% sand and have loamy sand or sandy loam textures.
- Group C: Soils in this group have moderately high runoff potential when thoroughly wet. Water transmission through the soil is somewhat restricted. Group C soils typically have between 20 and 40% clay and less than 50% sand and have loam, silt loam, sandy clay loam, clay loam, and silty clay loam textures.
- Group D: Soils in this group have high runoff potential when thoroughly wet. Water movement through the soil is restricted or very restricted. Group D soils typically have greater than 40% percent clay, less than 50% sand, and have clayey textures.

3.3 Land Use/Land Cover Maps

The land use/land cover maps of the study area were prepared using the satellite data of LISS-III sensor mounted on IRS-P6. The satellite data has a resolution of 23.5 m and is capable of recording in four different bands in the spectral range of 0.52–1.70 µm. This range corresponds to the visible as well as the near-infrared portions of the spectrum. LISS-III images for 2003 and 2010 were obtained from National Remote Sensing Center (NRSC). The data was subjected to supervised maximum likelihood classification, and the results obtained are shown in Figs. 1 and 2 with area-wise details in Tables 1 and 2.

Table 1 Area-wise breakup of different land use/land cover classes for 2003

Land cover class	Area (km^2)	Percentage area
Built up	22	2.61
Water bodies	12	1.43
Dense vegetation	428	50.83
Cultivated without conservation	258	30.64
Barren land	122	14.4

Table 2 Area-wise breakup of different land use/land cover classes for 2010

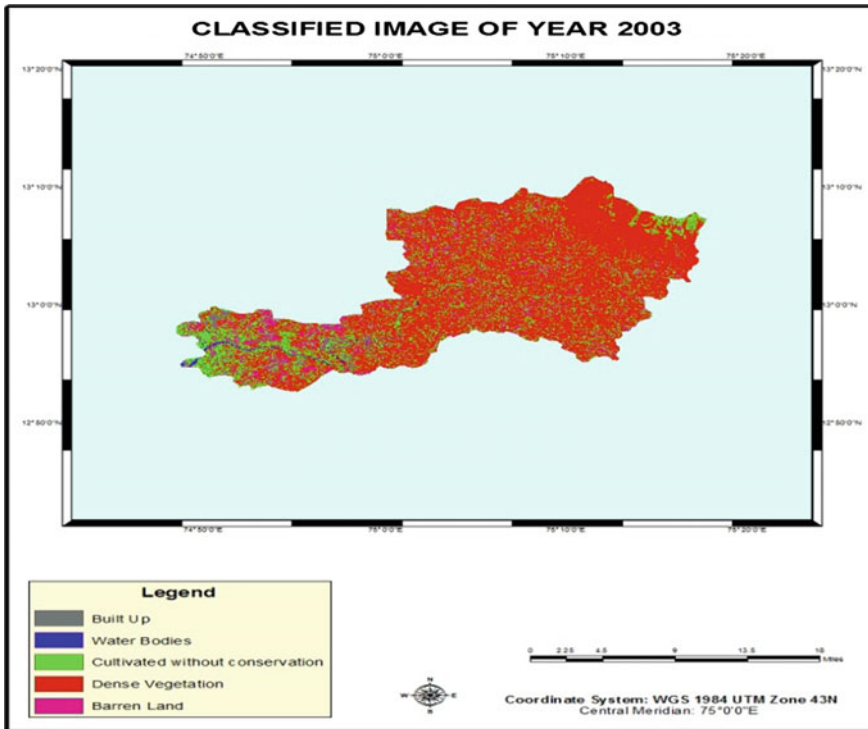| Land cover class	Area (km^2)	Percentage area
Built up	47	5.58
Water bodies	5	0.59
Dense vegetation	303	35.99
Cultivated without conservation	391	46.43
Barren land	96	11.41

Fig. 1 Classified image for 2003

An increase is seen in the land class of built-up area and cultivated land, whereas dense vegetation, barren lands, and water bodies have suffered decreases in their extents from 2003 to 2010.

The watershed was obtained by techniques of Automated Watershed Delineation. Due to more accuracy and dedicated scripts attributing to easy delineation, the method used in this study is the watershed delineation tool developed independently by GIS student Dwain Caldwell of GeoTREE University of Geography. The purpose of the script is to allow manual delineation of watershed boundaries. The tool requires a Digital Elevation Model and a pour point (i.e., outlet points for the watersheds you would like to delineate) raster dataset.

The Digital Elevation Model for the study area was downloaded from Bhuvan portal. The pour point used was Adoor gauging station. The results of the script include the basin, watershed, stream network, stream order network, filled DEMs, flow accumulation rasters, and flow direction rasters.
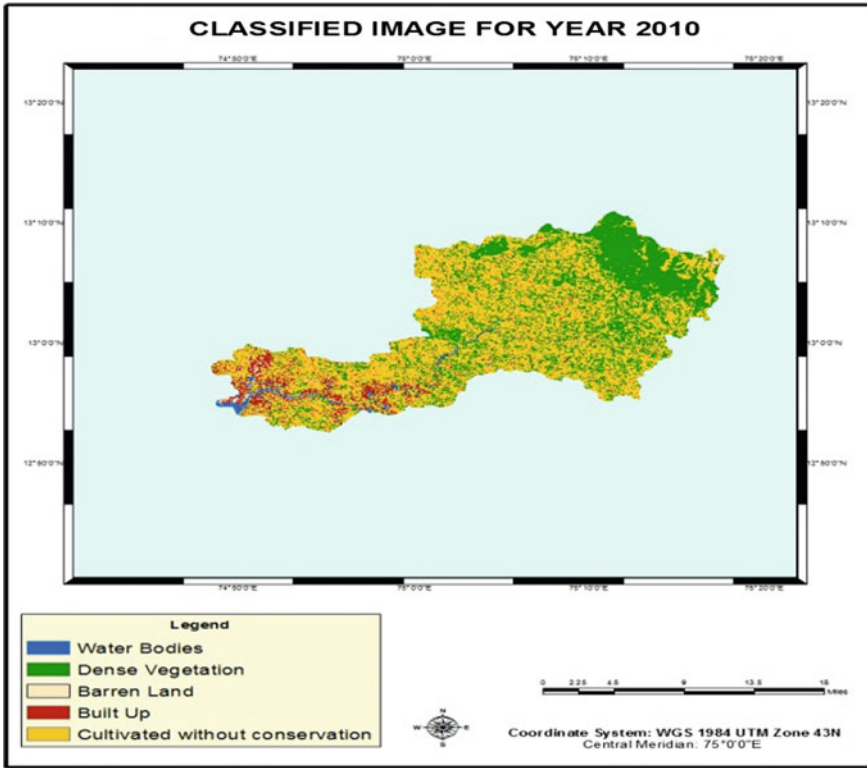
Fig. 2 Classified image for 2010

4 Results and Discussions

4.1 Runoff Estimation

Further, the classified images were intersected with the hydrological soil group map in order to determine the curve numbers for each class. The result produced was the curve number map of the entire area. The curve numbers are calculated by assuming the average Indian wetness conditions of AMC II.

Since curve number for each land use/land cover class has different value under different situations, area weighted curve number is calculated for each class. Following equation can be used to calculate weighted curve number [16, 22].

$$\text{Weighted Curve Number} = \frac{\sum_{i=1}^{n}(\text{CN}_i \times A_i)}{A} \tag{3}$$

Table 3 Area and hydrological soil group-wise breakdown of the different land use/land cover classes for 2003

Land cover class	Total area (km^2)	Hydrological soil group B		Hydrological soil group C		Hydrological soil group D	
		Area (km^2)	CN	Area (km^2)	CN	Area (km^2)	CN
Built up	22	5.7	98	5	98	11.3	98
Dense vegetation	428	22	57	340	71	66	78
Water bodies	12	8	100	3.3	100	0.7	100
Cultivated without conservation	258	57	71	158	78	43	81
Barren	122	9	61	97.5	74	15.5	80
						Weighted CN = 68.97	

Table 4 Area and hydrological soil group-wise breakdown of the different land use/land cover classes for 2010

Land cover class	Total area (km^2)	Hydrological soil group B		Hydrological soil group C		Hydrological soil group D	
		Area (km^2)	CN	Area (km^2)	CN	Area (km^2)	CN
Built Up	47	10.1	98	15.2	98	21.7	98
Dense vegetation	303	11	57	264	71	28	78
Water bodies	5	0.9	100	2.2	100	1.9	100
Cultivated without conservation	391	40	71	299	78	52	81
Barren	96	31	61	37	74	31	80
						Weighted CN = 74.53	

where

CN_i Curve number from 1 to any number n

A_i Area corresponding to CN_i

A Total area of the watershed

The results obtained are shown in Tables 3 and 4.

It is interesting to note the increase in the curve number from 68.97 in 2003 to 74.53 in 2010. The same can be attributed to the increase in the impermeable surfaces

in the form of built-up land and cultivated land. Both built-up land and cultivated land have increased by 53 and 34%, respectively, causing an uprise in the curve number.

After calculating the curve numbers, the runoff calculations can be done by employing SCS-CN method.

The general equation for the SCS curve number method is as follows:

$$Q = \frac{(P - \text{Ia})^2}{(P - \text{Ia}) + s} \tag{4}$$

where

Q Runoff (mm)
P Rainfall (mm)
Ia Initial abstraction
S Maximum potential retention after runoff begins

$$\text{Ia} = 0.3S \tag{5}$$

Therefore,

$$Q = \frac{(P - 0.3S)^2}{(P + 0.7S)} \tag{6}$$

$$S = \frac{25{,}400}{254 + \text{CN}} \tag{7}$$

The initial Eq. (4) is based on trends observed in data from collected sites; therefore, it is an empirical equation instead of a physically based equation. After further empirical evaluation of the trends in the database, the initial abstractions, Ia, could be defined as a percentage of S (5). With this assumption, the Eq. (6) could be written in a more simplified form with only three variables. The parameter CN is a transformation of S, and it is used to make interpolating, averaging, and weighting operations more linear (7).

The obtained results are in the form of runoff maps for the study area. The results indicate an increased runoff in 2010 as compared to 2003. Another interesting feature is the increased runoff in the month of November in 2010 as compared to the month of November in 2003. The predicted runoff values can be compared to the available stream gauging data of Adoor station obtained from India Water Resources Information System (IWRIS) portal version 4.0. The stream gauging data is first converted from total runoff to surface runoff by performing base flow separation by using Web-Based Hydrograph Analysis Tool (WHAT) available at https://engineering.purdue.edu/~what/.

The obtained results are shown in Table 5 and Figs. 3, 4.

Table 5 Comparison of available observed data of surface runoff and the predicted values

Month	2003		2010	
	Observed discharge (m³/s)	Predicted discharge (m³/s)	Observed discharge (m³/s)	Predicted discharge (m³/s)
August	147	125.6	154.94	130
September	34.73	23.7	63.78	51.2
October	33.57	26.9	33.56	26.6
November	5.915	0	30.7	20.82

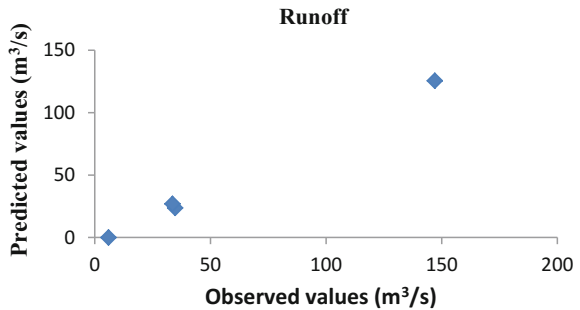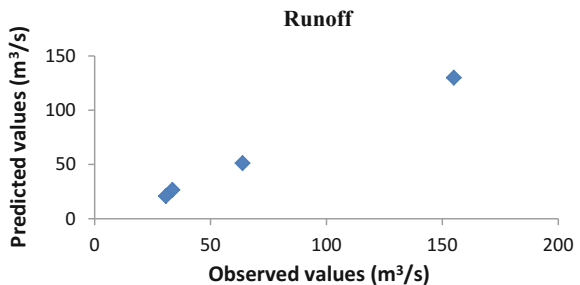**Fig. 3** Plot of observed runoff versus predicted runoff for 2003

Fig. 4 Plot of observed runoff versus predicted runoff for 2010

4.2 Calculating the Surface-Water Storage

Considerable surface water bodies were extracted from the classification images of the respected years. These polygons provided the spatial location and the area of the water bodies. The depth required for volume calculation was actuated by the 3-D profile of the study area, which was generated earlier, as shown in Figures 6.7 and 6.8. The polygon features were overlayed on the TIN of the study area, and the volume was found out by "Calculate Polygon" tool available in 3-D analyst toolset in ARC GIS 10.1. From these polygons, volume was calculated as shown in Tables 6, 7 and Fig. 5.

Also the total amount of incoming runoff is available for this storage volume. Now for the water balance equation, the two parameters, i.e., the runoff input and

Table 6 Calculated volume and surface area of the visible water bodies

Year	Calculated volume (m^3)	Surface area (m^2)
2003	23552.2896	3,100,515
2010	1366.032806	849,756

Table 7 Total runoff generated and the total storage volume available for years 2003 and 2010

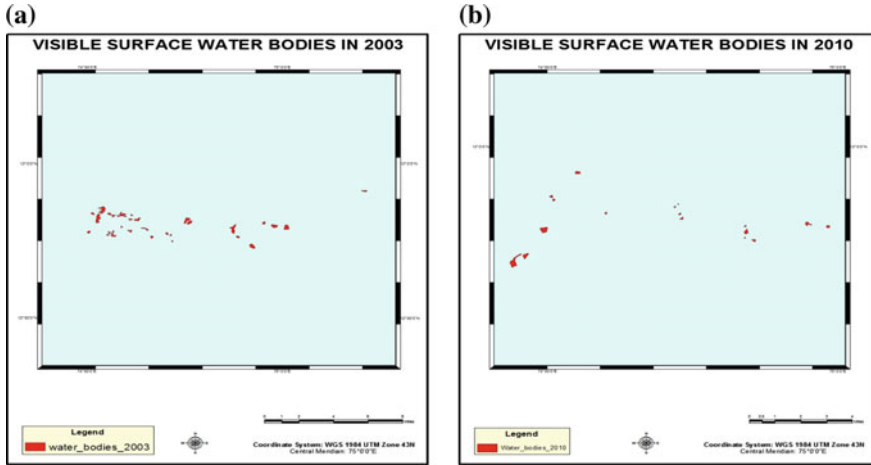| Year	Calculated volume (m^3)	Total runoff (m^3/s)
2003	3794.535572	16622.12
2010	1366.032806	30929.94

Fig. 5 Visible water bodies. **a** In 2003 and **b** in 2010

the storage volume, are known. The total runoff in 2003 and 2010 along with their storage volumes is represented in the following table.

It is observed that despite an increase in the total runoff in the 2010, there is steep decrease in the storage volume available for that runoff. The storage volume has decreased by 36%.

5 Conclusions

An attempt was made to assess the changes in the wetland storage by taking into account the two important aspects of the water balance equation, i.e., the surface-water inflow and the changes in storage. The surface-water inflow was estimated using SCS-CN method using moderate resolution LISS-III data. The resolution of the satellite data hampers the accuracy of the classification of the image into various land use/land cover classes. The classified images of the study years, i.e., 2003 and 2010, demonstrate the effect of increasing anthropogenic activities in the study area.

It can be duly noted by the fact that the built-up area has increased by 53% over the course of 7 years of the study. In the same time frame, the cultivated land including pastures and groves has seen an increase of 37%. It is also noted that the volume to the surface storage in the study area has decreased by 36% over the time frame of 7 years, whereas over the same time frame the runoff generated has increased. A major of portion these mentioned surface water bodies are the wetlands in the study area. Wetlands are well known to absorb the effects of excess runoff and help in preventing floods. But the current situation certainly points to a grave condition where the storage available for the absorption of runoff may not be enough to wary the effects of incoming runoff. This may lead to the constant flooding of low-lying areas and urban settlements. Therefore, an immediate need stems from the situation to protect and promote wetlands in the region.

References

1. Dhawale, A.W.: Runoff estimation for Darewadi Watershed using RS and GIS. Int. J. Recent Technol. Eng. **1**, 6 (2013)
2. Pandey, A., Dabral, P.P.: Estimation of runoff for hilly catchment using satellite data. J. Indian Soc. Remote Sens. **32**, 2 (2004)
3. Black, P.E.: Watershed Hydrology, vol. 2, pp. 231–236. Ann Arbor Press Inc., Chelsea (1996)
4. Brodie, R.S., Hostetler, S.: A review of techniques for analysing base flow from stream hydrographs. J. Am. Water Resour. Assoc. **53**(8), 579–663 (2010)
5. Prakasa Rao, B.S., Pernaidu, P., Amminedu, E., Rao, T.V., Sathi Devi, K., Jagadeeswara Rao, P., Srinivas, N., Bhaskara Rao, N.: Run-off and flood estimation in Krishna River delta using remote sensing and GIS. J. Indian Geophys. Union **15**(2), 101–112 (2011)
6. Chapman, T.G., Maxwell, A.I.: Baseflow separation—comparison of numerical methods with tracer experiments. Hydrological and Water Resources Symposium, Institution of Engineers Australia, Hobart, pp. 539–545
7. Ramakrishnan, D., Bandyopdhyay, A., Kusuma, K.N.: SCS-CN and GIS based approach for identifying potential water harvesting sites in the Kali Watershed, Mahi River Basin, India. J. Earth Syst. Sci. **118**(4), 355–368 (2009)
8. Furey, P., Gupta, V.K.: A physically based filter for separating base flow from streamflow time series. Water Resour. Res. **37**, 2709–2722 (2001)
9. Gonzales, A.L., Nonner, J., Heijkers, J., Uhlenbrook, S.: Comparison of different base flow separation methods in a lowland catchment. Hydrol. Earth Syst. Sci. **13**, 2055–2068 (2009)
10. Rouhania, H., Malekianb, A.: Automated methods for estimating base flow from stream flow records in a semi arid watershed. DESERT **17**, 203–209 (2012)
11. Adornado, H.A., Yoshida, M.: GIS-based watershed analysis and surface run-off estimation using curve number (CN) value. J. Environ. Hydrol. **18**, 1–10 (2010)
12. Arnold, J.G., Allen, P.M.: Automated methods for estimating base flow and ground water recharge from stream flow records. J. Am. Water Resour. Assoc. **35**(2), 411–424 (1999)
13. Arnold, J.G., Allen, P.M., Muttiah, R., Bernhardt, G.: Automated base flow separation and recession analysis techniques. Ground Water **33**(6), 1010–1018 (1995)
14. Mishra, S.K., Jain, M.K., Bhunya, P.K., Singh, V.P.: Field applicability of the SCS-CN-based Mishra-Singh general model and its variants. J. Water Resour. Manag. **19**, 37–62 (2006)
15. Sundar Kumar, P.: Estimation of rainfall-runoff of the Vijayawada City by SCSCN method using remote sensing and GIS. **1**(11), 1–4 (2012)
16. Nayak, T., Verma, M.K., Hema Bindu, S.: SCS curve number method in Narmada Basin. Int. J. Geomat. Geosci. **3**(1) (2012)

17. Eckhardt, K.: Analytical sensitivity analysis of a two parameter recursive digital base flow separation filter. Hydrol. Earth Syst. Sci. **16**, 451–455 (2012)
18. Latha, M., Rajendran, M., Murugappan, A.: Comparison of GIS based SCS-CN and strange table method of rainfall-runoff models for Veeranam Tank, Tamil Nadu, India. Int. J. Sci. Eng. Res. **3**(10) (2012)
19. Lim, K.J., Engel, B.A., Tang, Z., Choi, J., Kim, K.-S., Muthukrishnan, S., Tripathy, D.: Automated web GIS based hydrograph analysis tool. WHAT. J. Am. Water Resour. Assoc. **41**(6), 1407–1416 (2005)
20. National Engineering Handbook: United States Department of Agriculture, Part 630 Hydrology (2007)
21. Gupta, P.K., Panigrahy, S.: Predicting the spatio-temporal run-off generation in India using remotely sensed input and soil conservation service curve number method. Curr. Sci. **95**(11), 1580–1588 (2008)
22. Chow, V.T., Maidment, D.R., Mays, L.W.: Applied Hydrology. Tata McGraw-Hill Publications. New York (2010)
23. Zhan, X., Huang, M.-L.: ArcCN-Runoff: an ArcGIS tool for generating curve number and runoff maps. Environ. Model. Softw. **19**, 875–887 (2004)